The effect of antimony on the interfaces of cast AlSi–SiC composites

A. BARDAL
SINTEF Applied Physics, N-7034 Trondheim, and Department of Physics, University of Trondheim-NTH, Norway

When the matrix alloy of an AlSi7Mg–SiC composite has been modified with antimony, the wetting properties of the system deteriorate. Using transmission electron microscopy and microanalysis it was found that this is probably related to the formation of a film-like amorphous antimony-rich oxide at the matrix–silicon carbide interfaces. Associated with this compound are pores at the interfaces. The film-like compound is generally intermixed with magnesium–aluminium spinel crystallites at the interfaces and with the neighbouring matrix. No antimony-rich phase is found away from the interfaces.

1. Introduction

To modify the eutectic silicon particles of aluminium–silicon alloys, elements such as sodium, strontium or antimony are often added to the alloys. Theories explaining the effect usually deal with the modification by sodium [1, 2]. The exact mechanism by which antimony exerts its modifying action is not known, although it is believed that the twinning mechanism by which the silicon grows is poisoned [2, 3]. While sodium or strontium modification may be more common, antimony has the advantage of maintaining the modifying effect after remelting of the alloy and after heat treatments [4, 5].

When an antimony-modified alloy is used as the matrix material of a cast aluminium–silicon carbide composite, the properties deteriorate. The melt becomes viscous; the wetting is poor. The resulting material has much lower strength than the unmodified composite, and also lower ductility. The strength is, in fact, lower than for the unreinforced modified and unmodified alloys.

In this work composites of an antimony-modified AlSi7Mg alloy were studied by optical microscopy and scanning (SEM), transmission (TEM) and scanning transmission (STEM) electron microscopy. In particular TEM characterization of the matrix–silicon carbide interface was emphasized. For reference the unreinforced antimony-modified alloy and a composite of the unmodified alloy were also studied.

2. Materials and methods

The materials were produced by Hydro Aluminium, Sunndalsøra, Norway, by stirring silicon carbide particles into the aluminium melt before casting. Specimens for microstructural characterization were made from remelted ingots of this material. The composites contained 12–13 vol % SiC particles of average size 20 μm, and the modified aluminium alloy used for the matrix contained 7.2% Si, 0.6% Mg, 0.5% Fe, 0.11% Ti and 0.17% Sb, as measured by the manufacturer.

TEM specimens were prepared using spark erosion, mechanical polishing, dimple grinding and ion milling. Owing to possible reactions with the magnesium in the materials, water was avoided during the final steps of preparation.

The TEM characterization was done using a Philips CM-30 TEM/STEM equipped with an energy dispersive spectrometer (EDS) and a parallel electron energy loss spectrometer (EELS). The highest accelerating voltage of the instrument is 300 kV, giving a line resolution of less than 0.2 nm. EDS quantification was carried out using experimentally determined k-factors and assuming the foils to be thin enough for absorption and fluorescence corrections to be omitted.

3. Results and discussion

In addition to the antimony-modified composite, two reference materials were studied. The unreinforced antimony-modified alloy was studied in the TEM; no antimony-rich phase was found. The composite made from the unmodified alloy was studied optically, with SEM and TEM. Except from the antimony-containing phases and microstructural characteristics related to these, the microstructure as well as the phases found in the modified and unmodified composites are similar. All micrographs shown below are from the modified composite.

Prior to TEM characterization of the modified composite, an overview of the distribution of reinforcing silicon carbide particles and other phases was obtained using SEM, microprobe analysis and optical microscopy. The low-magnification optical micrograph of Fig. 1 shows that the distribution of silicon
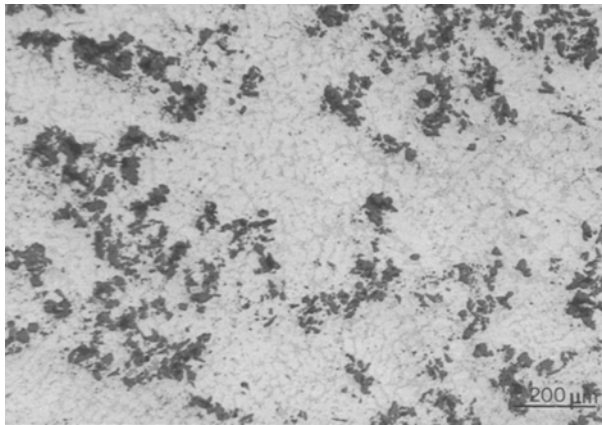
Figure 1 Optical micrograph showing inhomogeneous distribution of silicon carbide (dark). A network of eutectic silicon (grey) can be seen in the matrix.
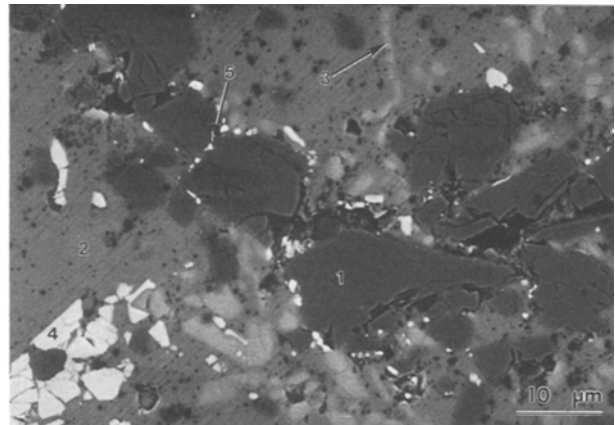
Figure 2 SEM image showing various phases containing (1) silicon and carbon; (2) aluminium, (3) silicon, (4) iron and (5) antimony.

carbide is not homogeneous. The lighter grey areas where no silicon carbide is present can have sizes up to hundreds of micrometres. A network of eutectic silicon particles is seen in the matrix.

The scanning electron micrograph in Fig. 2 shows a variety of phases of different appearance. The back-scattered electron image shows atomic number contrast, with the brighter areas corresponding to heavier elements. By means of wavelength dispersive (WDS) X-ray mapping using the microprobe, the elements present in the larger particles could be identified. The use of WDS instead of EDS allows for the detection of the light elements carbon and oxygen.

Five different phases were found in the SEM/microprobe images:

1. dark grey particles containing silicon and carbon: silicon carbide;
2. aluminium matrix, medium grey;
3. lighter grey particles containing silicon only;
4. large white particles containing iron;
5. smaller white particles containing antimony.

Black areas in between clustered silicon carbide are pores.

The silicon and iron- and antimony-rich particles tend to cluster around the silicon carbide. This probably reflects the fact that the silicon carbide tends to be pushed into the melt which solidifies last and which is enriched with the alloying elements.

By means of the TEM, a closer look was taken at the interfaces between the matrix and the silicon carbide. The superior spatial resolution compared to SEM allows for the identification of smaller particles and thin interfacial layers. The various phases found with the microprobe and the SEM could also be identified more accurately.

The major impurity is iron which in this alloy is expected [2] to be present in the form of the inter-metallics $FeSiAl_5$ and $FeMg_3Si_6Al_8$. Both phases were indeed found in the composites. The iron-rich phases could be found in the matrix and at the matrix–silicon carbide interfaces. Furthermore, in the as-cast condition one should expect some Mg_2Si in the matrix. This

was also found in the form of the rod-shaped β' modification. The Mg_2Si was not associated with matrix–silicon carbide interfaces. The equilibrium β-phase of Mg_2Si was not found.

EDS X-ray maps obtained using the STEM mode of the CM-30 reveal that the antimony has segregated to the silicon carbide interfaces. Both at interfaces between silicon carbide and the aluminium matrix and between silicon carbide and large eutectic silicon particles, an antimony-rich layer is observed, whereas the material away from the interfaces shows no antimony. Fig. 3 shows an example of this. Fig. 3a is a bright-field image from a silicon carbide–silicon interface. A layer of about 100 nm thickness is seen at the interface, which is viewed approximately edge-on. It is also noticed that the silicon particle is heavily twinned (Fig. 3a and b), a result of the eutectic growth process. A closer look at this interfacial layer shows that it is not a single continuous phase, it is in fact composed of many small crystallites. Controlled tilting of single particles within these can be done if the particles are not too small, and the zone axis diffraction patterns thus obtained reveal the $MgAl_2O_4$ spinel phase. This is, in fact, the only phase which has been identified within the layers of this kind.

The set of EDS X-ray maps from this interface which is shown in Fig. 3c–f shows that the interfacial layer contains aluminium, magnesium and antimony. The matrix, which can be seen in the upper left corner, contains some magnesium in addition to the aluminium. No antimony is present here.

The interfacial layer probably consists of more or less stoichiometric spinel crystallites which may contain some antimony, embedded in some amorphous oxide phase, possibly a silica-alumina mixture with some magnesium and antimony. The reduction of surface silica on the silicon carbide by the molten metal can lead to these oxide phases.

Fig. 4 is from a different silicon–silicon carbide interface where EDS maps again show that antimony, magnesium and aluminium is confined to an inter-facial layer. Singly distributed spinel crystallites are seen in Fig. 4a, while the high-resolution image of
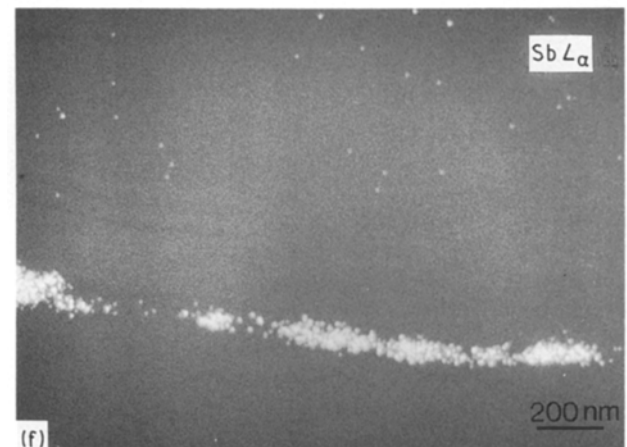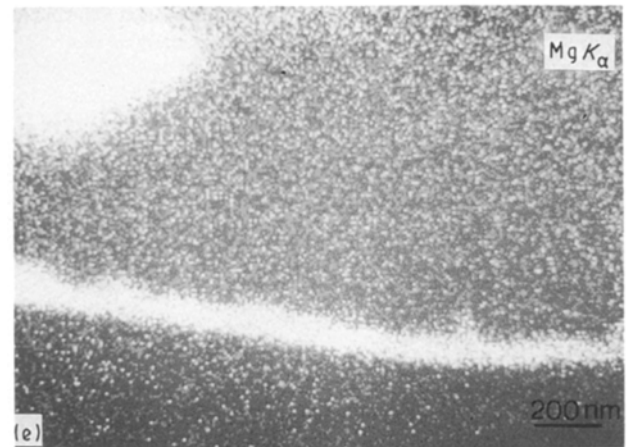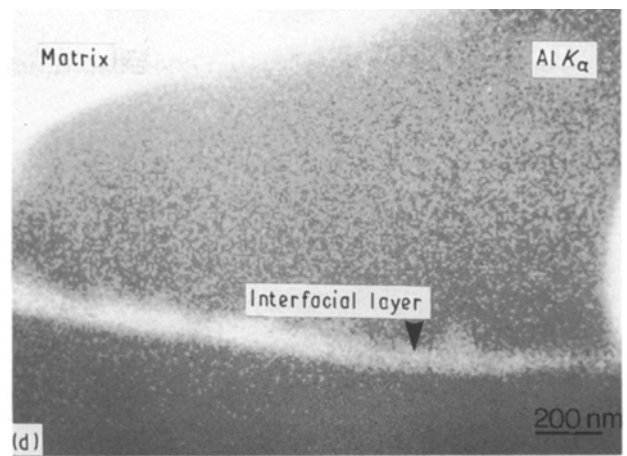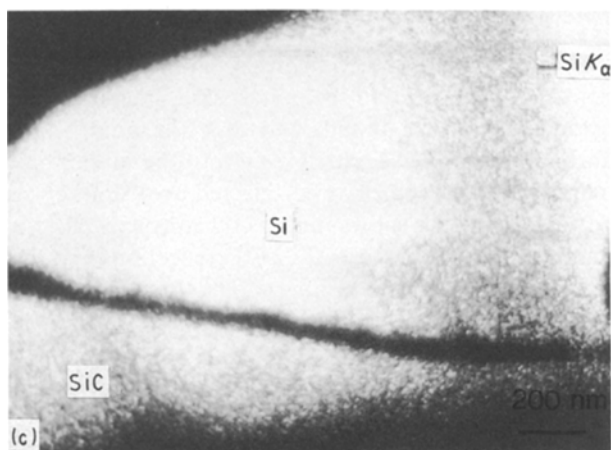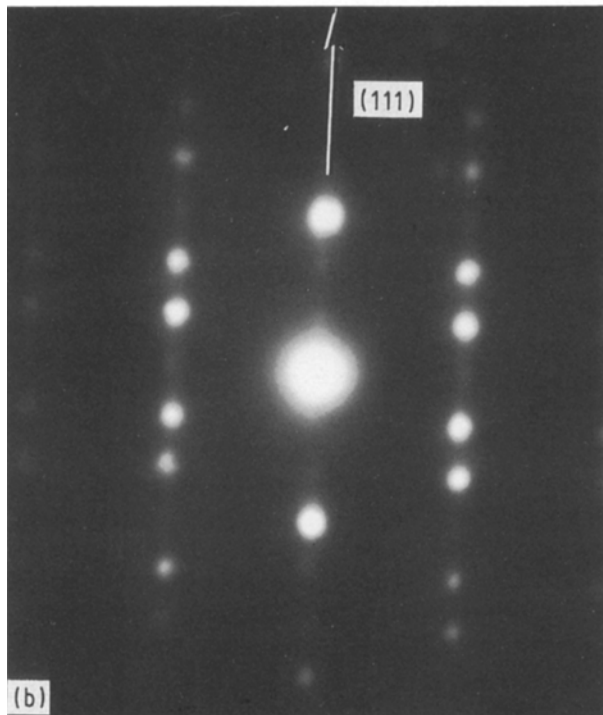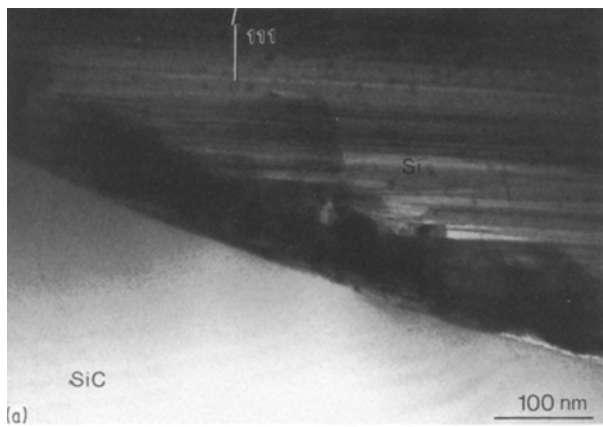
Figure 3 Interfacial layer between silicon and silicon carbide. The layer is composed of crystallites that index as magnesium–aluminium spinels. (a) Bright-field image and (b) $\langle 1\,1\,0 \rangle$ diffraction pattern from the silicon particle showing twinning along $\langle 1\,1\,1 \rangle$. The EDS maps (c–f) from the interfacial region show the layer to contain antimony, magnesium and aluminium. The brighter areas of the maps correspond to the higher concentrations.

Fig. 4b suggests that an amorphous phase is indeed present at the interface between silicon carbide, silicon and spinel.

The presence of antimony-containing layers where the silicon has grown to form interfaces with the silicon carbide, raises the question of whether antimony is also found at interfaces between silicon and the aluminium matrix. This was checked, and no antimony was detected. These interfaces are, in fact, very clean, no second phases were found.

So far, only interfaces with fairly low amounts of antimony have been displayed. At these interfaces a closer identification of the form in which the antimony is present is difficult. A film-like phase that is really
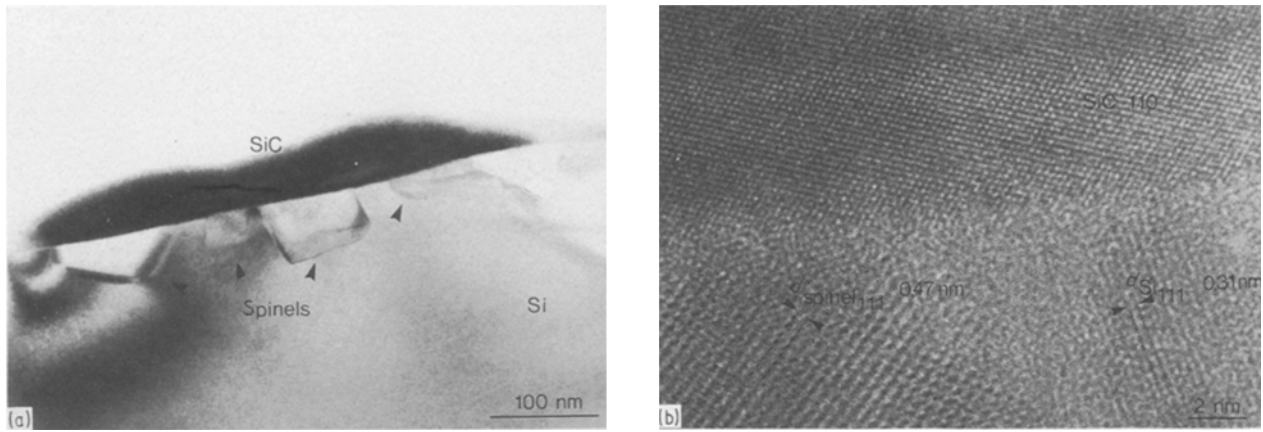
Figure 4 The silicon–silicon carbide interface where EDS maps show antimony, magnesium and aluminium enrichment. (a) Bright-field image showing singly distributed spinel crystallites along the interface. (b) High-resolution image showing an amorphous layer between the silicon carbide, silicon and spinel. The silicon carbide is viewed along the $\langle 1\,1\,0 \rangle$ zone axis direction.
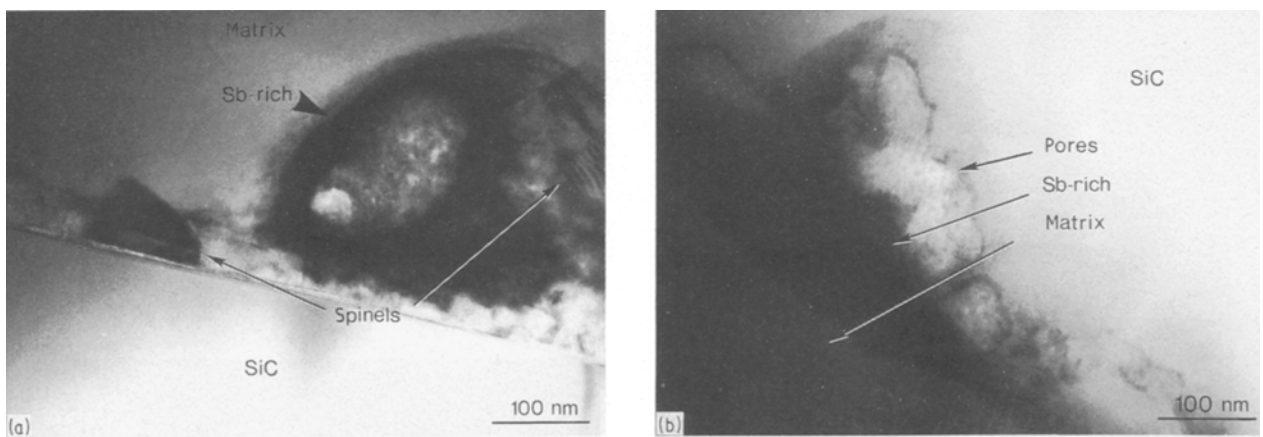

Figure 5 A film-like antimony-rich phase that folds around the matrix and spinel crystallites (a), or stretches along the matrix–silicon carbide interfaces (b). Associated with this phase are pores, sometimes covered by film (b).

rich in antimony is, however, present at many of the interfaces in the material. This phase, shown in Fig. 5, seems to stretch along the interfaces or fold around the matrix or spinel crystallites.

The film-like phase is often accompanied by larger pores, indicative of incomplete wetting. It shows no diffraction contrast changes upon tilting, and diffraction patterns reveal the haloes characteristic of an amorphous material. The correlation distance corresponding to the radii of these haloes is approximately 0.3 nm.

To attempt to determine the composition of the antimony-rich phase, EDS point analyses were carried out. As the phase is intermixed with smaller spinel crystallites and matrix, these will often contribute to the EDS spectra. After carrying out a large number of measurements it seems clear that there is no distinct ratio between the antimony and the aluminium or magnesium concentrations.

Fig. 6 shows an area where EDS measurements were carried out. The bright-field image of Fig. 6a shows an interfacial layer between the silicon carbide and the aluminium matrix. This layer is crystalline and indexes as spinel; the EDS measurements, how-

ever, shows a strong aluminium excess compared to the stoichiometric spinel. They also show a few atomic per cent antimony. On the matrix side, smaller spinel crystallites can be found, and also the amorphous antimony-rich phase, partly covering the aluminium matrix and the spinels. The selected-area diffraction pattern of Fig. 6b shows the $\langle 1\,1\,0 \rangle$ zone axis pattern of one of the spinels, two Al $\langle 2\,0\,0 \rangle$ reflections and the halo from the amorphous phase. The three EDS spectra displayed in Fig. 6c–e are acquired at slightly different positions in the matrix area, and show varying ratios between the antimony and the other elements. Quantification of the spectrum in Fig. 6e gives more than 80 at % Sb. The Mg:Al ratio of Fig. 6d is close to 1:2 (atomic) whereas Fig. 6c has an excess of aluminium, probably due to overlap with and thus contribution from the matrix. Spinel particles can again be seen intermixed with the dark phase, and pores are present towards the interfacial spinel-like phase.

The fact that the antimony-rich phase is only found associated with the silicon carbide suggests that the phase is an oxide, formed during production of the composite by reaction between the liquid metal and
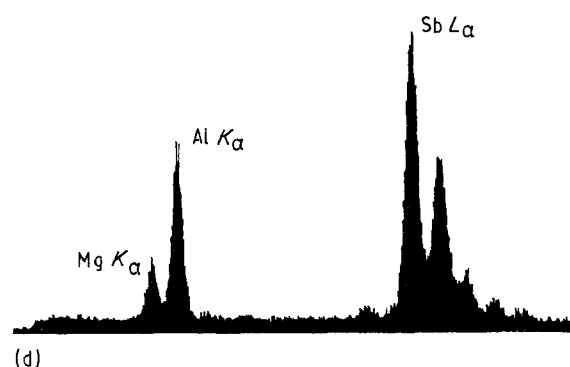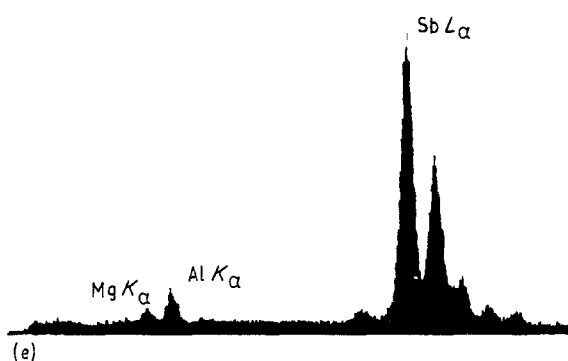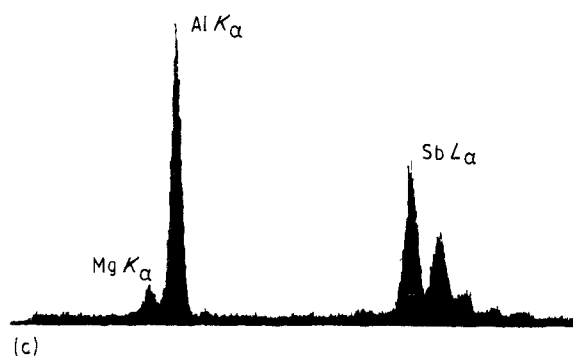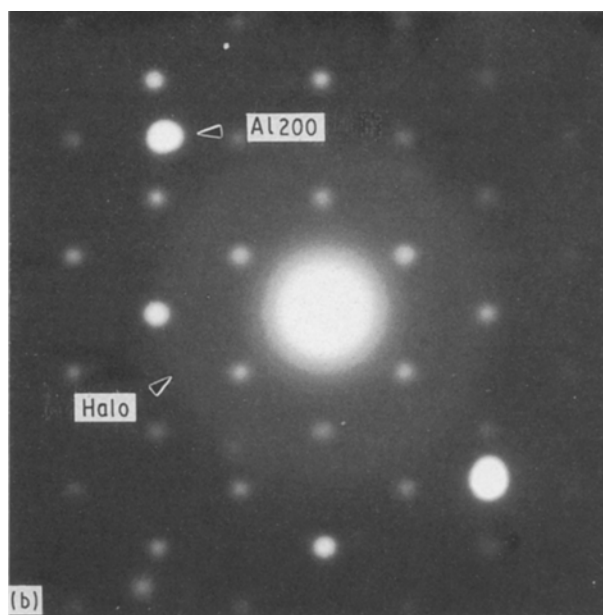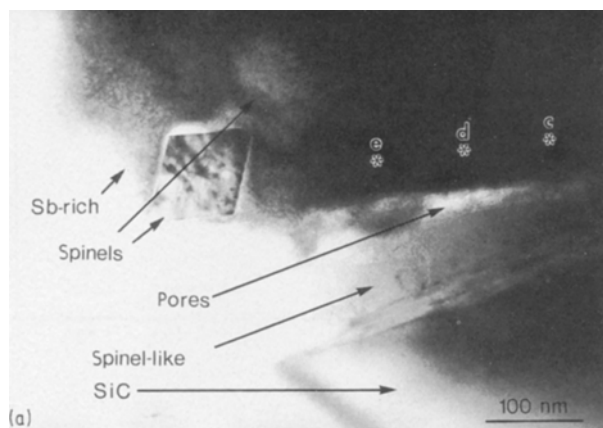
Figure 6 The matrix–silicon carbide interface. (a) Bright-field TEM image showing SiC particle, crystalline spinel-like interfacial layer, and matrix with spinel crystallites partially covered by amorphous antimony-rich phase. The positions where EDS spectra were taken shown in Fig. 6c–e are also indicated. (b) Diffraction pattern from the area around the small regularly shaped spinel, close to the spinel $\langle 1\,1\,0 \rangle$ zone axis, and showing Al $\langle 2\,0\,0 \rangle$ reflections and a halo from the amorphous antimony-rich phase. (c–e) EDS spectra showing varying Sb:Al:Mg concentration ratios.

surface silica on the silicon carbide. The possible presence of oxygen in this phase was checked by means of electron energy loss spectroscopy (EELS).

In the ion-milled TEM specimens it proved difficult to find areas that were thin enough to study the fine structure of the EELS spectra. A TEM sample was therefore prepared by butanol extraction [6, 7] where the aluminium matrix is dissolved and the remaining silicon carbide and interfacial phases are deposited on holey carbon film for examination. With this method it was possible to isolate a thin particle of the amorphous antimony-rich phase. The antimony-rich particle is shown in Fig. 7 along with its diffraction pattern and an EDS spectrum showing strong AlK_α and SbL_α lines. Quantitative EDS shows that the Al:Sb ratio is very close to 1 (atomic).

Fig. 8 shows an EELS spectrum from this particle. As seen from the plasmon loss region of Fig. 8a the particle is thin, and plasmon scattering–ionization deconvolution should thus not be necessary for studying the fine structure of the edges. The region of

the spectrum seen in Fig. 8b and c, the latter with the background removed, shows the superimposed $SbM_{4,5}$ and OK edges at 527 and 532 eV, respectively. This nearly complete overlap of the $SbM_{4,5}$ and OK edges is a slightly complicating factor when trying to detect oxygen in the antimony-rich phase.

The OK edge can, however, be detected due to the delayed maximum of the $SbM_{4,5}$ edge [8, 9]. Although the fine structure of the OK edges may vary for different metal oxides, they have the same qualitative feature of a steep and abruptly rising edge at the edge onset energy of 532 eV and an edge maximum below 550 eV. The $SbM_{4,5}$ edges, on the other hand, rise very slowly from the onset energy at 527 eV and only reach a maximum between 600 and 650 eV.

From the shapes of the $SbM_{4,5}$ and OK edges of the acquired EELS spectra we can tell that oxygen is present in considerable amounts. Owing to the overlap of the edges, it is not easy to determine the O:Sb ratio by means of EELS. EDS with an ultrathin window detector could be used to obtain quantitative
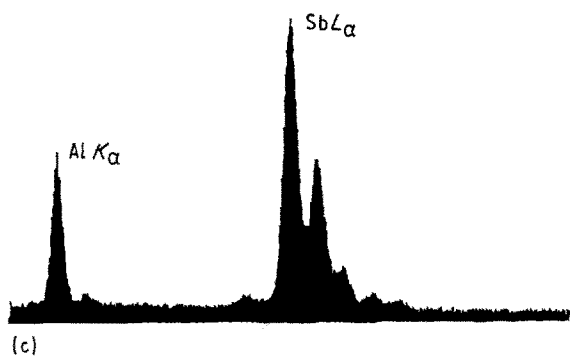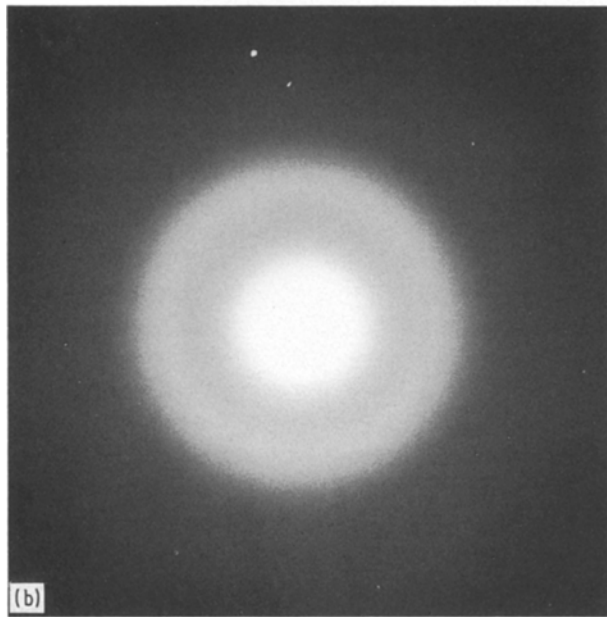
Figure 8 EELS spectrum from the antimony-rich particle seen in Fig. 7. (a) Low-loss region, (b) superimposed $SbM_{4,5}$ (527 eV) and OK (532 eV) edges. (c) Superimposed $SbM_{4,5}$ and OK edges after removal of background.

Figure 7 An amorphous particle containing antimony, aluminium and oxygen. (a) Bright-field image, (b) diffraction pattern, (c) EDS spectrum showing strong aluminium and antimony lines. Quantification gives an Al:Sb ratio close to 1 (atomic).

results for the oxygen content of the antimony-rich phase. This was, however, not available on the instrument used.

In support of the possibility of an antimony oxide is the work of Standage and Gani [10]. During the studies of the reaction between aluminium melt and silica, it was noted that the addition of bismuth or antimony to the melt markedly reduced the rate of reaction. 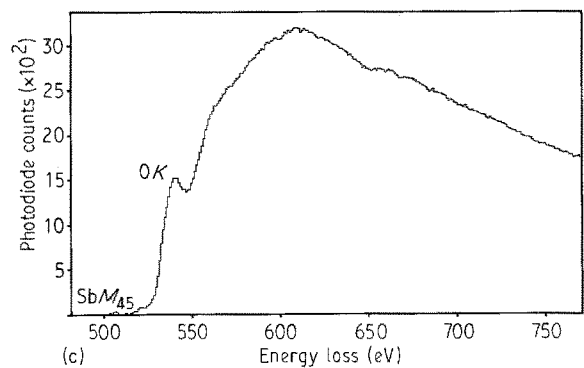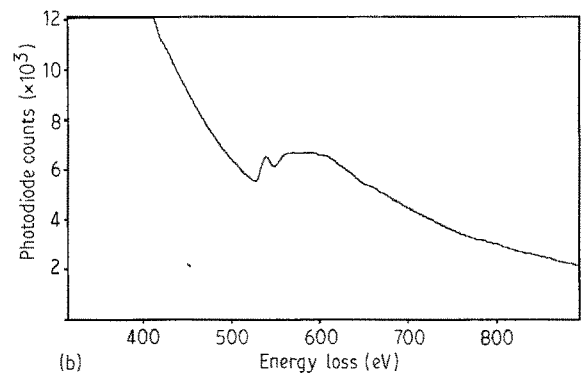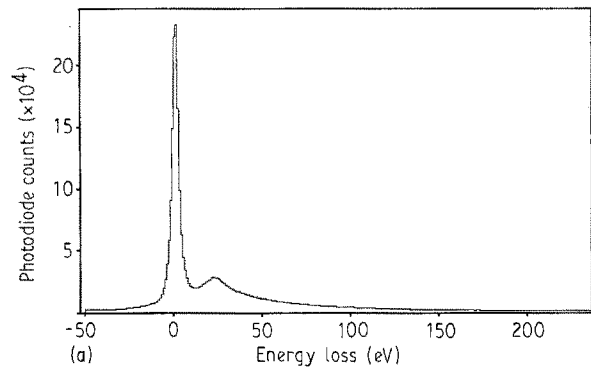The authors proposed that these elements form a lamellar compound with oxygen and water absorbed on the silica surface, this compound controlling the reaction kinetics.

4. Conclusion

The poor wetting and bad properties of the antimony-modified composite seem to be related to the presence of antimony-rich phases at the silicon carbide interfaces and pores associated with these phases. Antimony has been found at all investigated matrix–silicon carbide interfaces and has not been found in the matrix away from the interfaces. It is found in relatively low concentrations in layers along the interfaces together with or within magnesium–aluminium spinels, possibly nonstoichiometric. It is also found in high concentrations in some amorphous phase of film-like appearance, stretching along the

interface or folding around the matrix and spinel crystallites. The two appearances of antimony may be the same phase which is present in different quantities. The phase with high antimony content is an oxide, and it contains varying amounts of aluminium. This oxide is likely to have been formed during production of the composite, through reaction of the molten metal with the surface silica on the silicon carbide.

Acknowledgements

References

1. A. HELLAWELL, *Prog. Mater. Sci.* **15** (1973) 3.

2. L. F. MONDOLFO, "Aluminium Alloys" (Butterworths, London, 1976) pp. 672–82.
3. A. I. TELLI and S. E. KISAKÜREK, *Scripta Metall.* **20** (1986) 1657.
4. E. BRUNHUBER, *Giesserei-praxis* (1981) 4, 61.
5. A. VOKÁLKOVÁ and V. KABICKÝ, *Prakt. Met.* **21** (1984) 133.
6. C. J. SIMENSEN, P. FARTUM and A. ANDERSEN, *Fresenius Z. Anal. Chem.* **319** (1984) 286.
7. B. R. HENRIKSEN, *J. Microsc.* **160** (1990) 327.
8. R. F. EGERTON, "Electron Energy Loss Spectroscopy in the Electron Microscope" (Plenum Press, New York, 1986) Ch. 3.6.1.
9. C. C. AHN and O. L. KRIVANEK, "EELS Atlas" (Arizona State University/Gatan, Tempe, 1983).
10. A. E. STANDAGE and M. S. GANI, *J. Amer. Ceram. Soc.* **50** (1967) 101.